Cellular and molecular mechanisms of arrhythmias in cardiac fibrosis and beyond : from symptoms to substrates towards solutions

Askar, S.F.A.

Cellular and Molecular Mechanisms of Arrhythmias in Cardiac Fibrosis and Beyond:

From Symptoms to Substrates towards Solutions

Chapter V

Prolongation of Minimal Action Potential Duration in Sustained Fibrillation Decreases Complexity by Transient Destabilization

Brian O. Bingen, MD; **Saïd F. A. Askar, MSc**; Martin J. Schalij, MD, PhD; Ivan V. Kazbanov, Msc; Dirk L. Ypey, PhD; Alexander V. Panfilov, PhD; Daniël A. Pijnappels, PhD.

Adapted from Cardiovasc Res 2013;97:161-170

Abstract:

Aims: Sustained ventricular fibrillation (VF) is maintained by multiple stable rotors. Destabilization of sustained VF could be beneficial by affecting VF complexity (defined by the number of rotors). However, underlying mechanisms affecting VF stability are poorly understood. Therefore this study aimed to correlate changes in arrhythmia complexity with changes in specific electrophysiological parameters, allowing to search for novel factors and underlying mechanisms affecting stability of sustained VF.

Methods & Results: Neonatal rat ventricular cardiomyocyte monolayers, and Langendorff-perfused adult rat hearts, were exposed to increasing dosages of the gap junctional uncoupler 2-aminoethoxydiphenyl borate (2-APB) to induce arrhythmias. Ion channel blockers/openers were added to study effects on VF stability. Electrophysiological parameters were assessed by optical-mapping and patch-clamp techniques.

Arrhythmia complexity in cardiomyocyte cultures increased with increasing dosages of 2-APB (n>38), leading to sustained VF: 0.0±0.1 phase singularities/cm^2 in controls vs. 0.0±0.1, 1.0±0.9, 3.3±3.2, 11.0±10.1 and 54.3±21.7 in 5,10,15,20 and 25µmol/L 2-APB, respectively. Arrhythmia complexity inversely correlated with wavelength. Lengthening of wavelength during fibrillation could only be induced by agents ($BaCl_2$/BayK8644) increasing APD at maximal activation frequencies (minimal APD); 123±32%/117±24% of control. Minimal APD prolongation led to transient VF destabilization, shown by critical wave front collision leading to rotor termination, followed by significant decreases in VF complexity and activation frequency (52%/37%). These key findings were reproduced *ex vivo* in rat hearts (n=6 per group).

Conclusions: These results show that stability of sustained fibrillation is regulated by minimal APD. Minimal APD prolongation leads to transient destabilization of fibrillation, ultimately decreasing VF complexity, thereby providing novel insights into anti-fibrillatory mechanisms.

Introduction

Ventricular fibrillation (VF) is the most common cause of sudden cardiac death.[1] Treatment of VF has vastly improved over the past years, mainly through progress in engineering strategies that resulted in defibrillating devices. However, while defibrillators can have a significant effect on survival, the majority of VF victims are not defibrillator candidates and at least 50% have VF as their first symptom of heart problems.[2] This is indicative of an unabated need to expand the current understanding of mechanisms underlying VF stability and termination.

One of the factors which can underpin the initiation of VF is gap junction remodeling. It is widely accepted that gap junctions are redistributed or down regulated following myocardial infarction, in cardiac hypertrophy and other causes of cardiomyopathy.[3] Such reorganization of gap junctions is associated with the onset of malignant ventricular tachyarrhythmias.[3-5]

After initiation, VF progresses through several distinct activation pattern phases, of which the hindmost are characterized by a reduction in the number of new rotor formations, reduced rotor meandering and increased spatiotemporal periodicity,[6-10] leading to a more organized and stable form of fibrillation. Affecting the stability of sustained VF may lead to a lower complexity of VF (estimated by the number of phase singularities per cm^2), but the underlying mechanisms are poorly understood. Traditionally, the fibrillatory aspect of conduction as well as arrhythmia complexity during fast VF is believed to be determined by conduction velocity (CV), action potential duration (APD), APD restitution slope and wavelength (the product of CV and APD).[11-13] However, considering the distinctive VF activation patterns, the importance of these factors could differ significantly during the different phases of VF. Furthermore, while data on the first phases after VF initiation are abundant,[11,14-16] data on sustained VF are scarce.[5] Therefore, a new *in vitro* and *ex vivo* model of sustained VF was developed that enabled to correlate a systematic and controllable increase in arrhythmia complexity with changes in specific electrophysiological parameters. Subsequent pharmacological modification of key parameters was used to search for novel factors affecting the stability of sustained VF and thereby unravel the underlying anti-fibrillatory mechanisms.

Methods

All animal experiments were approved by the Animal Experiments Committee of the Leiden University Medical Center and conform to the Guide for the Care and Use of Laboratory Animals as stated by the US National Institutes of Health. A more detailed description can be found in the Supplemental Material.

Cell isolation and culture

Neonatal rat ventricular myocytes were isolated by collagenase digestion as described previously,[17] Animals were anaesthetized with 4–5% isoflurane inhalation anesthesia. Adequate anesthesia was assured by the absence of reflexes prior to rapid heart excision. Ventricles were minced and digested using collagenase (Worthington, Lakewood, NJ, USA) and DNAse (Sigma-Aldrich, St. Louis, MO, USA). After isolation, cells were plated out isotropically on fibronectin-coated, round glass coverslips (15 mm) at a cell density of 2-8x10^5 cells/well in 24-well plates (Corning Life Sciences, Amsterdam, the Netherlands). To prevent overgrowth of remaining cardiac fibroblasts, proliferation was inhibited by Mitomycin-C (Sigma-Aldrich, St. Louis, MO, USA) treatment at day 1, as described previously.[17] All cultures were refreshed daily with DMEM/HAM's F10 in a 1:1 mixture with 5% HS and cultured in a humidified incubator at 37º C and 5% CO_2.

Immunocytological analyses

Cultures were stained for Connexin40 (Sigma), Connexin43 (Santa Cruz Biotechnologies, Santa Cruz, CA, USA) and Connexin45 (Santa Cruz) to assess presence of gap junctional proteins, and for active caspase-3 (Abcam, Cambridge, MA, USA) to assess the number of apoptotic cells. Images of cultures were taken and quantified using dedicated software (ImageJ, National Institutes of Health, USA).

Optical mapping of myocardial cultures

At day 4 of culture, propagation of action potentials was investigated on a whole-culture scale by optical mapping using di-4-anepps (Sigma) as voltage sensitive dye, as described previously.[17] Cells were incubated with 2-APB in 5 different concentrations (5, 10, 15, 20 and 25 μM) for 20±2 minutes, targeting Connexin43, Connexin45 and Connexin40[18,19] to induce arrhythmias of increasing complexity, while vehicle-treated cultures were used as controls. Data analysis, construction of activation maps and stripe analysis (e.g. plotting of optical signal amplitude against time, at the maximal diameter of a culture or short and long axis of whole heart) were performed with specialized software (Brainvision Analyze 1101, Brainvision Inc, Tokyo, Japan) after pixel signals were averaged with 8 of its nearest neighbors, minimizing noise-artifacts. CV in cultures with uniform or reentrant activation patterns was calculated perpendicular to the activation wave front, between two 3 by 3 pixel grids typically spaced 2-8 mm apart. CV, activation frequency, minimal APD (during

maximal paced activation frequency) and 1Hz APD were determined at 6 different locations equally distributed throughout the culture and averaged before further analysis. APD was determined at 80% of repolarization (APD_{80}) because of the rat action potential shape. Wavelength was calculated by the product of average CV and an APD_{80} (for uniform propagation) or reentrant cycle length[12]. Arrhythmia complexity was defined as the number of phase singularities per cm^2, determined by using the phase space method[20] and correlated with CV, APD_{80} and wavelength in order to identify potential targets that can be modified to affect VF stability and thereby reduce VF complexity. As a result of the outcome of this correlation, appropriate drugs (3 µmol/L nitrendipine (Sigma), 1 mmol/L sotalol (Sigma), 0.5 mmol/L $BaCl_2$ (Merck, Darmstadt, Germany) or 1 µmol/L BayK8644 (Sigma)) were administered to 2-APB treated and control cultures to modify these targets and study the effects on arrhythmia complexity.

Assessment of arrhythmia complexity

Arrhythmia complexity in cardiomyocyte cultures was defined as the number of phase singularities per cm^2. To quantify the number of phase singularities the phase space approach was used.[20] Time series analyses using the empirical mode decomposition method and the Hilbert transform were used to determine the phase.[21] Data was smoothed by Gaussian filtering with a spatial size of 5 pixels (approx. 0.75 mm) and a temporal size of 5 frames (30 ms). Subsequently, a discrete Fourier transform was performed for each pixel over the full time series. By using the Fourier spectra the dominant frequency was determined. After that a band-pass filter was applied to each time series removing low and high frequencies. Next, the local extrema for the time series were found using a half of the inverse dominant frequency as the window size. Local maxima (and local minima) were interconnected by a piece-wise linear curve and their mean curve was subtracted from the corresponding time series. Then by using the Hilbert transform of the resulting time series the phase $\varphi_{ij}(t)$ for every pixel (i, j) at the moment of time t was determined as

$$\varphi_{ij}(t) = \operatorname{atan2}\left(I_{ij}(t), H\left[I_{ij}(t)\right]\right)$$

Where $I_{ij}(t)$ is the filtered and detrended intensity of the optical mapping signal for the pixel (i, j) at the moment t and $H[\cdot]$ denotes the Hilbert transform.

The topological charge of the area Ω is determined by

$$n(\Omega) = \frac{1}{2\pi} \oint_{\partial\Omega} \operatorname{grad} \varphi \mathrm{d}\boldsymbol{l}$$

where the integral is taken along the oriented boundary of Ω. For each pixel (i, j) we defined Ω_{ij} as a square around it with the side of 3 pixels. Thus the integral was approximated by the sum of 9 finite differences.

$$n(\Omega_{ij}) = \frac{1}{2\pi}\left(\left(\varphi_{i-1,j-1} - \varphi_{i-1,j}\right) + \left(\varphi_{i-1,j} - \varphi_{i-1,j+1}\right) + \cdots + \left(\varphi_{i,j-1} - \varphi_{i-1,j-1}\right)\right)$$

The overall algorithm was implemented in the OCaml programming language using the GTK+ toolkit for visualization.
Meandering of the phase singularities was defined as the maximal straight distance covered by the same phase singularity within 6 s of optical mapping.

Whole-cell patch-clamp

Whole-cell measurements were performed in spontaneously active cultures plated out in a density of $4x10^5$ cells/well in 24 well plates as described previously.[17] At day 4 of culture, current-clamp experiments were performed in CMCs at 25°C using an L/M-PC patch-clamp amplifier (3 kHz filtering) (List-Medical, Darmstadt, Germany). To study the effects of 2-APB on electrophysiological properties of CMCs, 25 µM 2-APB (Tocris Bioscience, Bristol, United Kingdom) was incubated for 20 min prior to measurements.

Ex vivo experiments

For *ex vivo* experiments, female adult Wistar rats of 6±3 months were anesthetized through inhalation of 3-5% isoflurane and received 400 IE of heparin intraperitoneally. After confirmation of adequate anesthesia by absence of pain reflexes, beating hearts were rapidly excised and immediately submersed in cold Tyrode solution comprised of (in mM) NaCl 130, $CaCl_2$ 1.8, KCl 4.0, $MgCl_2$ 1.0, NaH_2PO_4 1.2, $NaHCO_3$ 24 and glucose 5.5 at pH 7.4. Subsequently, the aorta was canulated and retrogradely perfused with Tyrode that was freshly oxygenated with carbogen (95% O_2, 5% CO_2) and supplemented with 20mM of 2,3-butanedione monoxime (BDM) to reduce motion artifacts, at a constant flow of 15±2 ml/min at 37° C using a modified Langendorff apparatus (AD instruments, Spechbach, Germany). Hearts were stained with 2 µM di-4-anepps by a 10 ml bolus injection into the bubble trap. The optical mapping camera was positioned facing the ventral surface of the heart, viewing equal portions of the left and the right ventricle during mapping. All hearts exhibited spontaneous sinus rhythm during initial acclimatization. Arrhythmia complexity was defined as the as the number of separate wave fronts present at the epicardial surface of the heart. The targets that were shown to affect arrhythmia complexity *in vitro* were modified by administration of 0.5 mM $BaCl_2$ to the perfusate for 10 minutes prior to measurements to confirm their *ex vivo* effects on arrhythmia complexity.

Statistical analysis

Statistical analyses were performed using SPSS11.0 for Windows (SPSS, Inc., Chicago, IL, USA). Data were compared with one-way ANOVA test with Bonferroni post-hoc correction if appropriate and expressed as mean±SD. Comparison between two groups was performed using a student t-test. Before and after comparisons were performed with a paired t-test. Differences were considered statistically significant if $P<0.05$. Non-linear regression curves were constructed by using a robust exponential two phase decay curve fit. Accuracy of these curves was expressed as the robust standard deviation of the residuals (RSDR).

Results

Cell culture characterization and the effect of gap junctional uncoupling by 2-APB

Immunocytological analysis of cultures by collagen-I and α-actinin double-staining, suitable for distinction between fibroblasts and CMCs,[17] showed that cultures consisted of 17.6±3.1% fibroblasts (n=6) (Supplemental Figure 1A). Fibroblasts were homogeneously spread across the culture. In addition, cultures showed expression of Connexin43 and Connexin45 as well as heterogeneous expression of Connexin40 in between CMCs, which are the targets for 2-APB,[18,19] as judged by immunocytological staining (Supplemental Figure 1B, 1C and 1D).

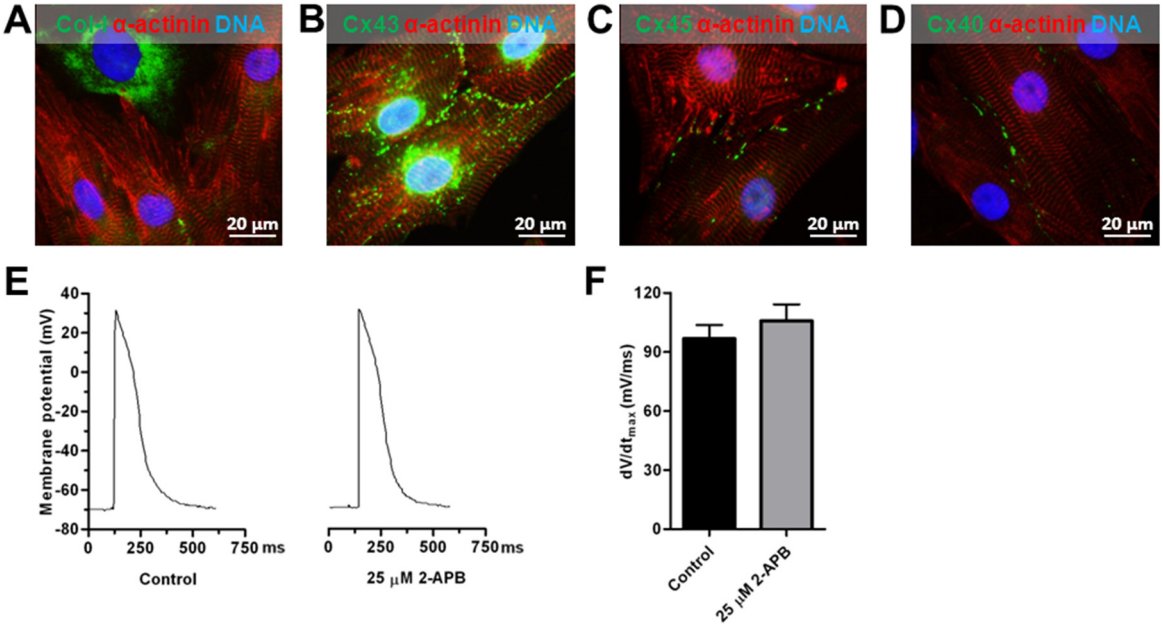

Supplemental Figure 1. *Cell culture characterization, gap junctional protein expression and modulation of gap junctional coupling*. (A) Immunocytological double-staining of α-actinin (red) and collagen-I (green), (B) Connexin43 (green), (C) Connexin45 (green) and (D) Connexin40. (E) Typical examples of membrane potential traces in control cultures and cultures treated with 25 µmol/L 2-APB and (F) Assessment of dV/dTmax.

2-APB causes stable multi-rotor tachyarrhythmias, resembling sustained VF, in a dose-dependent relation

During optical mapping, spontaneously active control cultures typically showed uniform and fast conduction (Figure 1A). However, after incubation with 2-APB, cultures showed a strong increase in the incidence of spontaneous reentrant tachyarrhythmias (Figure 1A and 1B). Furthermore, we observed a significant increase in the complexity of tachyarrhythmias, as

judged by the number of phase singularities per cm^2 with increasing dosages of 2-APB (Figure 1A, 1C and Supplemental movie 1). As a consequence of the increasing incidence of reentry with increasing 2-APB dosages (activation is higher during reentrant activation when compared to spontaneous uniform activation), average activation frequency was significantly increased after incubation with increasing dosages of 2-APB (Figure 1D). CV was dose-dependently decreased by treatment with 2-APB (Figure 1E). The decrease in CV remained apparent even when determined only during reentrant activation (Figure 1E, hatched subsets). Despite the high complexity of the tachyarrhythmias observed, the arrhythmias showed a high degree of stability that resembled sustained VF. In more detail, after initiation of reentry by treatment with 2-APB cultures showed a minimal extent of rotor meandering, which further decreased significantly with increasing 2-APB dosages (Supplemental Figure 3B). In addition, a relatively low number of fibrillating cultures showed new rotor formations, while all cultures showed minimal dispersion in optical signal amplitude as well as reentrant cycle length (Supplemental Figure 3 C-E), exemplified by stripe analysis of optical mapping recordings (Figure 1F).

The effect of gap junctional uncoupling by 2-APB

Treatment by 2-APB did not significantly change the AP morphology (Figure 1E), and dV/dT_{max} (Supplemental Figure 1F). Apoptosis was not increased in 2-APB treated cultures as judged by the expression of active caspase-3 (*P*=ns vs. control) (Supplemental Figure 2). Together these results suggest that the gap junction uncoupling agent 2-APB does not negatively affect cell excitability and viability.

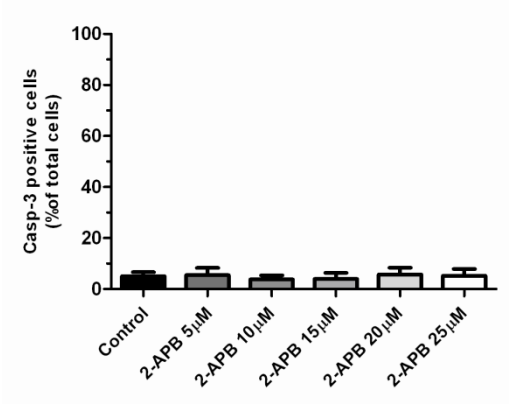

Supplemental Figure 2. *2-APB does not increase apoptosis in myocardial cultures. Quantification of apoptosis as judged by immunocytological staining of caspase-3 positive cells as a percentage of total cells (number of positive nuclei for Hoechst 33342 counterstaining).*

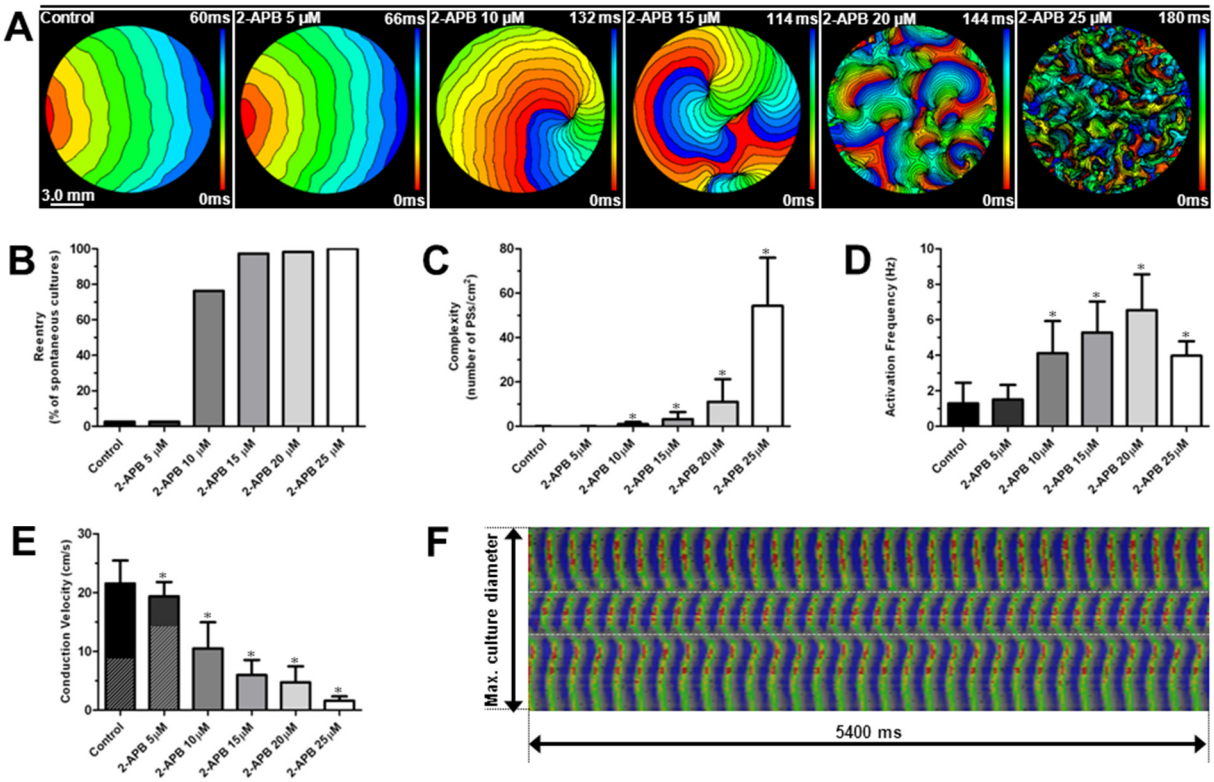

Figure 1. *(A) Activation maps (**6**ms isochronal spacing) of control cultures and 5-25µmol/L 2-APB treated cultures. (B) Quantification of reentry incidence, (C) complexity, (D) average activation frequency (both uniform and reentrant conduction included) and (E) CV in control cultures and 5-25µmol/L 2-APB treated cultures (n=38, n=38, n=39, n=39, n=61 and n=39 respectively). Hatched subsets indicate average CV during reentry in control and 5µmol/L 2-APB treated cultures (n=1 and 1). *: P<0.05 vs. control. (F) Typical line scan analysis across the diameter of a culture treated with 20µmol/L 2-APB (dotted line indicates rotor position).*

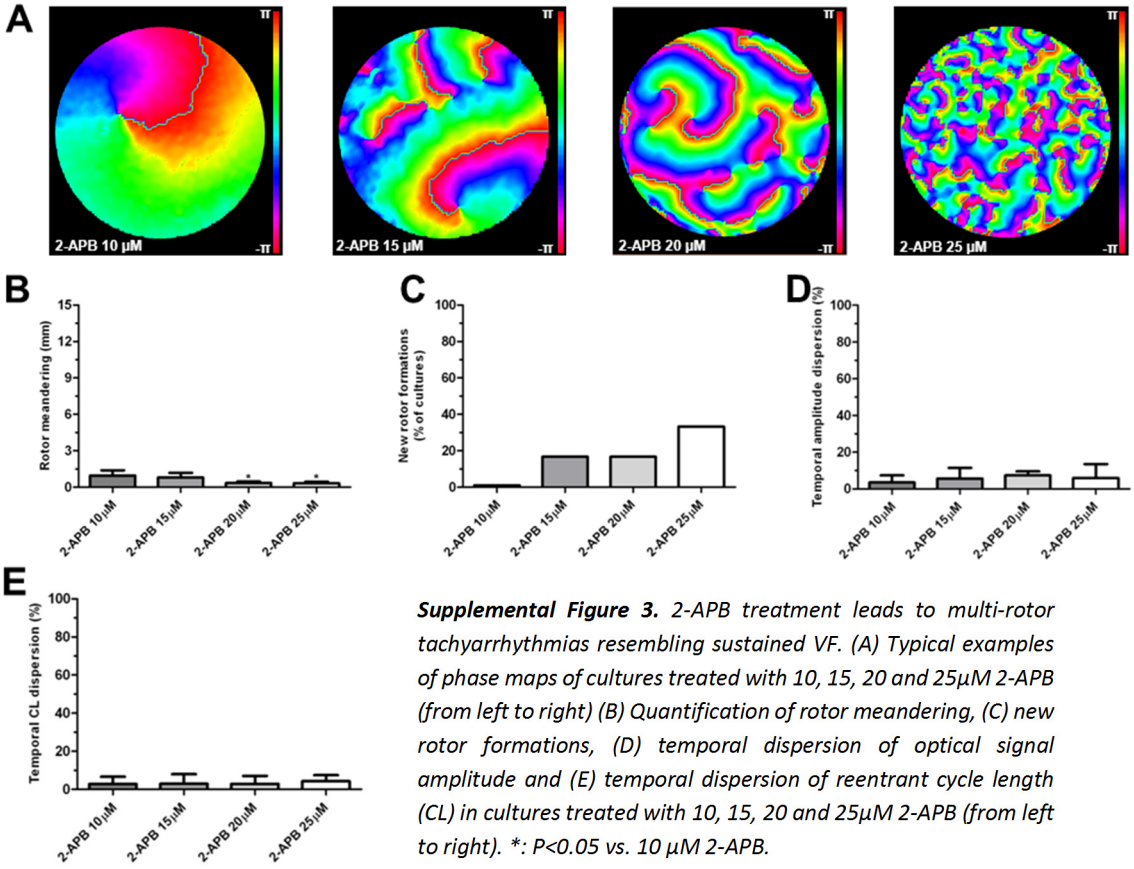

Supplemental Figure 3. *2-APB treatment leads to multi-rotor tachyarrhythmias resembling sustained VF. (A) Typical examples of phase maps of cultures treated with 10, 15, 20 and 25µM 2-APB (from left to right) (B) Quantification of rotor meandering, (C) new rotor formations, (D) temporal dispersion of optical signal amplitude and (E) temporal dispersion of reentrant cycle length (CL) in cultures treated with 10, 15, 20 and 25µM 2-APB (from left to right). *: P<0.05 vs. 10 µM 2-APB.*

Arrhythmia complexity increase is strongly related to wavelength shortening

To identify factors associated with increased arrhythmia complexity, the relationship between several electrophysiological parameters and complexity were investigated at variable 2-APB concentrations. As increasing 2-APB concentrations dose-dependently increased complexity, while at the same time decreasing CV, expectedly CV showed a strong hyperbolic-like relationship with complexity (RSDR=1.9) (Figure 2A). Furthermore, APD_{80} showed a weak inverse correlation with complexity in the low complexity range (Figure 2B). However, as at the highest 2-APB concentration the beating frequency decreases (Figure 1D), APD increases in cultures treated with 25µmol/L 2-APB. This slightly decreased the negative correlation between APD and complexity, while greatly increasing variation in APD. As wavelength is the product of CV and APD, wavelength shortening strongly related to complexity increases (RSDR=0.4) (Figure 2C). Together, these results support that inversely, complexity may be strongly diminished by increasing wavelength.

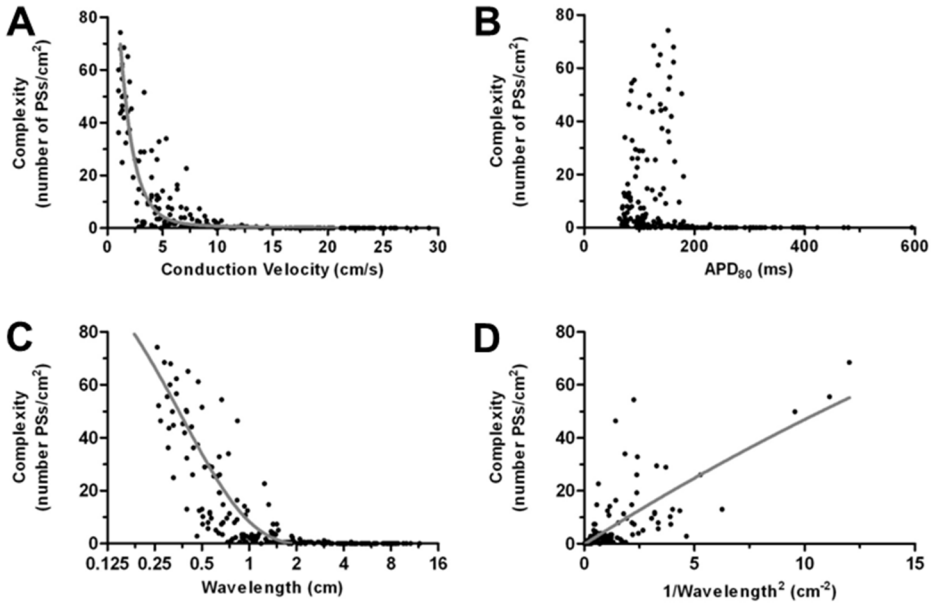

Figure 2. *Relationship between (A) CV and complexity, (B) APD_{80} and complexity, (C) wavelength and complexity (D) 1/[wavelength]^2 and complexity in control and 2-APB treated cultures (5-25µmol/L).*

Effects of pharmacological ion current modulators on 1Hz and minimal APD

To test whether arrhythmia complexity can be diminished by increasing wavelength, several ion channel modulators were selected, which according to their mechanism of action should have an effect on APD and wavelength. However, as fast activation, during fibrillation, can have an effect on activation and inactivation status of targeted ion channels,[22] the effect of the selected ion channel modulators might differ between fibrillation and normal uniform activation. Therefore, we assessed the effect of pharmacological ion channel modulation on APD at 1Hz electrical activation and at the minimal diastolic interval during 1-10Hz pacing (measuring minimal APD) in absence of reentrant circuits. As expected, nitrendipine, which inhibits I_{CaL}, significantly shortened the 1Hz APD by 28% (to 72±12%, P<0.05 vs. control) (Figure 3A and 3I), as well as minimal APD (to 84±14%, P<0.05 vs. control) (Figure 3E and 3J). Treatment with sotalol and $BaCl_2$ slowed repolarization and thus prolonged 1Hz APD (to 117±12% P<0.05 and 162±25% P<0.05 vs. control, respectively) (Figure 3B, 3C and 3I). However, the effect of sotalol on minimal APD was not significant, (Figure 3F and 3J), while $BaCl_2$ still had a significantly prolonging effect on APD during 10Hz pacing (to 145±9%, P<0.05 vs. control) (Figure 3G and 3J). Additionally, activation of I_{CaL} by Bayk8644 increased both 1Hz (to 168±13% P<0.05 vs. control) (Figure 3D and 3I) and minimal APD (to 133.7±9.6% P<0.05 vs. control) (Figure 3H and 3J) significantly.

Different effects of ion channel modulators on 2-APB induced fibrillation

In order to correlate the effects of selected ion channel modulators on minimal APD with their effects on the characteristics of fibrillation (i.e. APD, wavelength, stability, activation frequency and complexity), tachy-arrhythmic cultures induced by 2-APB were treated with nitrendipine, sotalol, $BaCl_2$ and BayK8644 (n>24 per agent).

In line with the previous, electrically stimulated experiments, APD_{80} was significantly decreased by nitrendipine throughout all 2-APB dosages, while APD was increased by both $BaCl_2$ and BayK8644. In contrast, sotalol did not affect APD significantly (Figure 4A, supplemental table 1). Wavelength was decreased significantly by nitrendipine treatment in the lowest concentration of 2-APB, although there was no significant effect in the other 2-APB dosages. In contrast, wavelength was significantly increased after $BaCl_2$ and BayK8644 treatment while sotalol did not significantly affect wavelength (Figure 4B, Supplemental Table 2). Interestingly, decreasing the APD with nitrendipine increased activation frequency of tachyarrhythmias. Conversely, lengthening of APD decreased activation frequency as seen after treatment with $BaCl_2$ and BayK8644 throughout all 2-APB dosages (Figure 4C, Supplemental Table 3). Sotalol induced a small but significant decrease in activation frequency in 15 and 20µmol/L 2-APB treated cultures only.

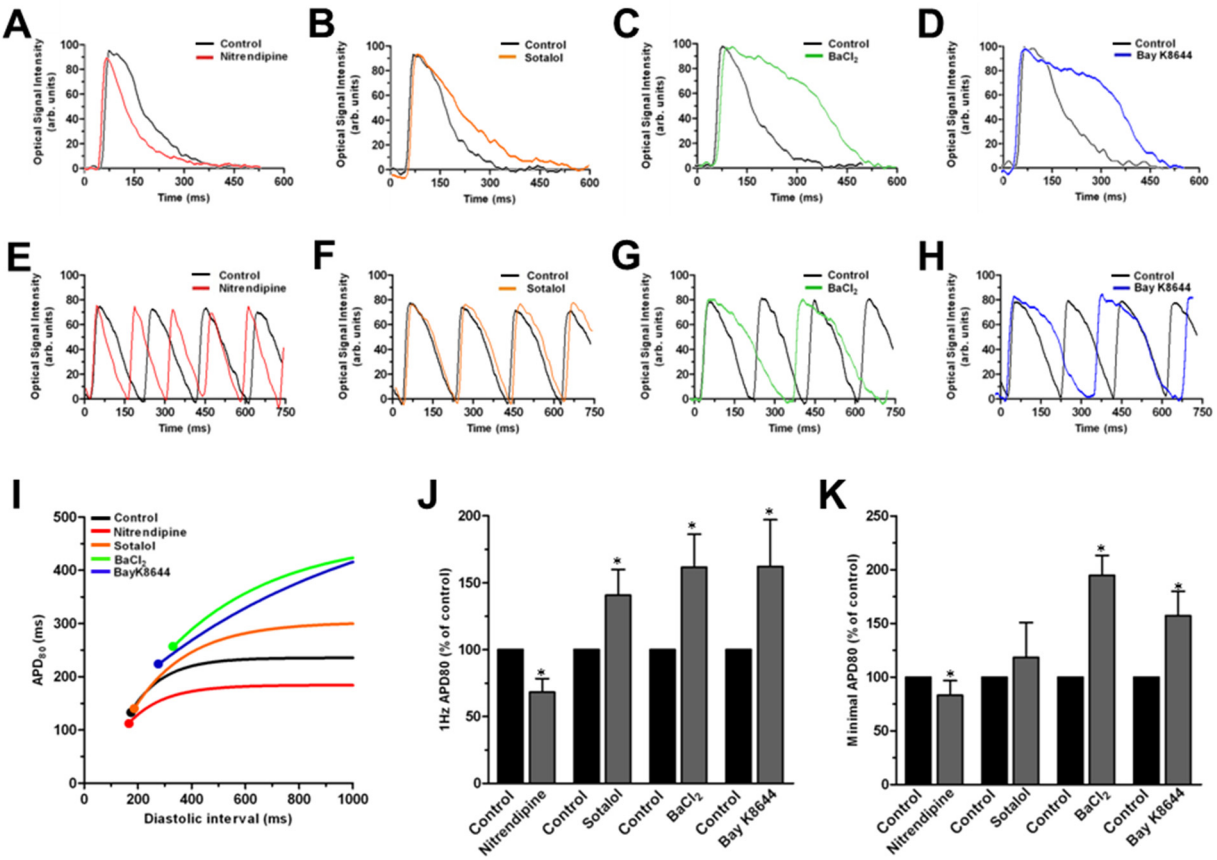

Figure 3. *Typical optical action potential records in control (black) and (A) nitrendipine (red), (B) sotalol (orange), (C) $BaCl_2$ (green) and (D) BayK8644 (blue) treated cultures illustrating treatment effects on 1Hz APD and minimal APD (E-H) and (I) APD restitution. Colored circles indicate the average minimal APD. Quantification of (J) 1Hz APD and (K) minimal APD before and after treatments. *: P<0.05 vs. control.*

The average complexity of conduction did not significantly alter after nitrendipine, while sotalol only had a small but significant effect on complexity in 25µmol/L 2-APB treated cultures. However, in $BaCl_2$ and BayK8644 treated cultures arrhythmia complexity was significantly lowered throughout all 2-APB concentrations except for the less complex arrhythmias after 10µmol/L 2-APB (Figure 4D, Supplemental Table 4). These results are indicative of the importance of minimal APD in decreasing and increasing complexity, through specific ion channel modulation.

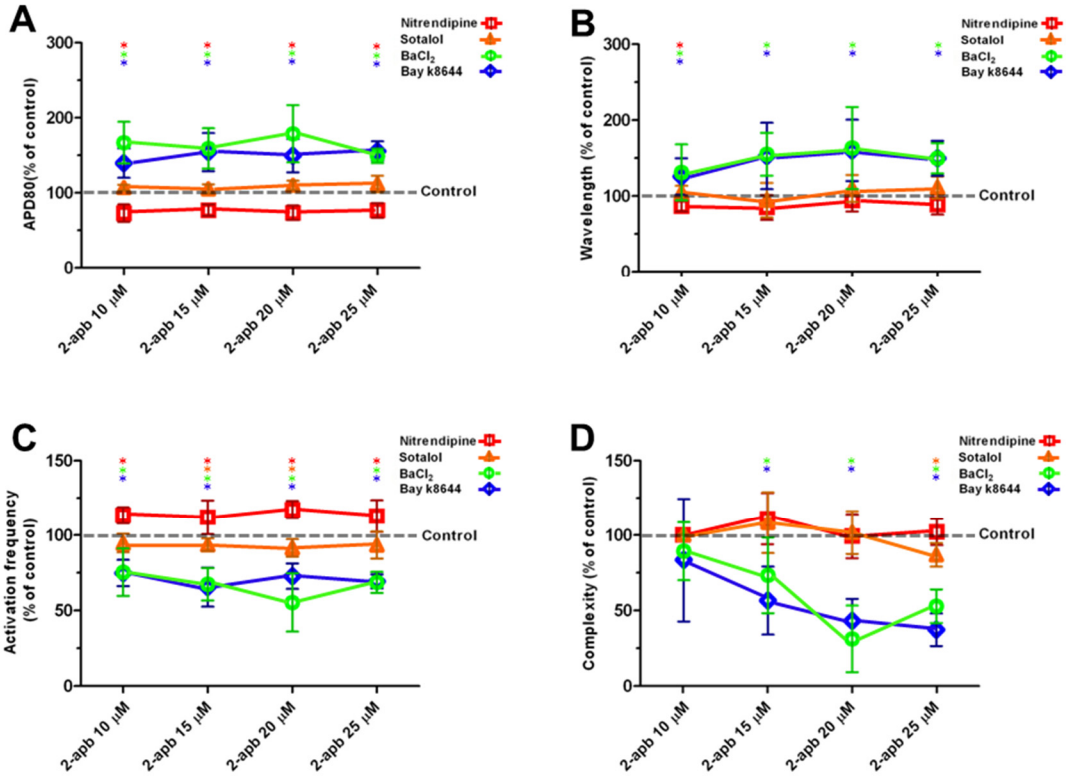

Figure 4. *(A) Quantification of APD, (B) wavelength, (C) activation frequency and (D) complexity after treatment with sotalol (orange), nitrendipine (red), $BaCl_2$ (green) and BayK8644 (blue). Dotted black lines indicate controls (prior to treatment set at 100%). *: P<0.05 vs. control.*

Mechanism of decrease in arrhythmia complexity by increase in minimal APD

Optical mapping through a permeable membrane during minimal APD prolongation by BayK8644 and $BaCl_2$ again showed that both substances decrease the number of rotors *in vitro* (Figure 5A). Prior to the addition of $BaCl_2$ or BayK8644, optical signal amplitude, spatial rotor distribution and rotor cycle lengths were highly stable (Figure 5B, D left). During incubation of $BaCl_2$ or BayK8644 transient instability in optical signal amplitude, spatial rotor distribution and rotor cycle length was induced (Figure 5B, D middle and Supplemental Figure 4A,B). Subsequently, a new equilibrium was formed, with increased optical signal amplitude, decreased number of rotors and stable but increased rotor cycle lengths (Figure 5B, D right and Supplemental Figure 4A,B). During incubation of $BaCl_2$ and BayK8644 this transient instability, which was mediated by an increase in wavelength, led to termination of neighboring rotors. Rotor termination resulted from critical collisions of wave fronts propagated from 2 different rotors, after which activation of that particular tissue is taken over by a separate pre-existing rotor, decreasing the total number of rotors (Figure 5C, 5D).

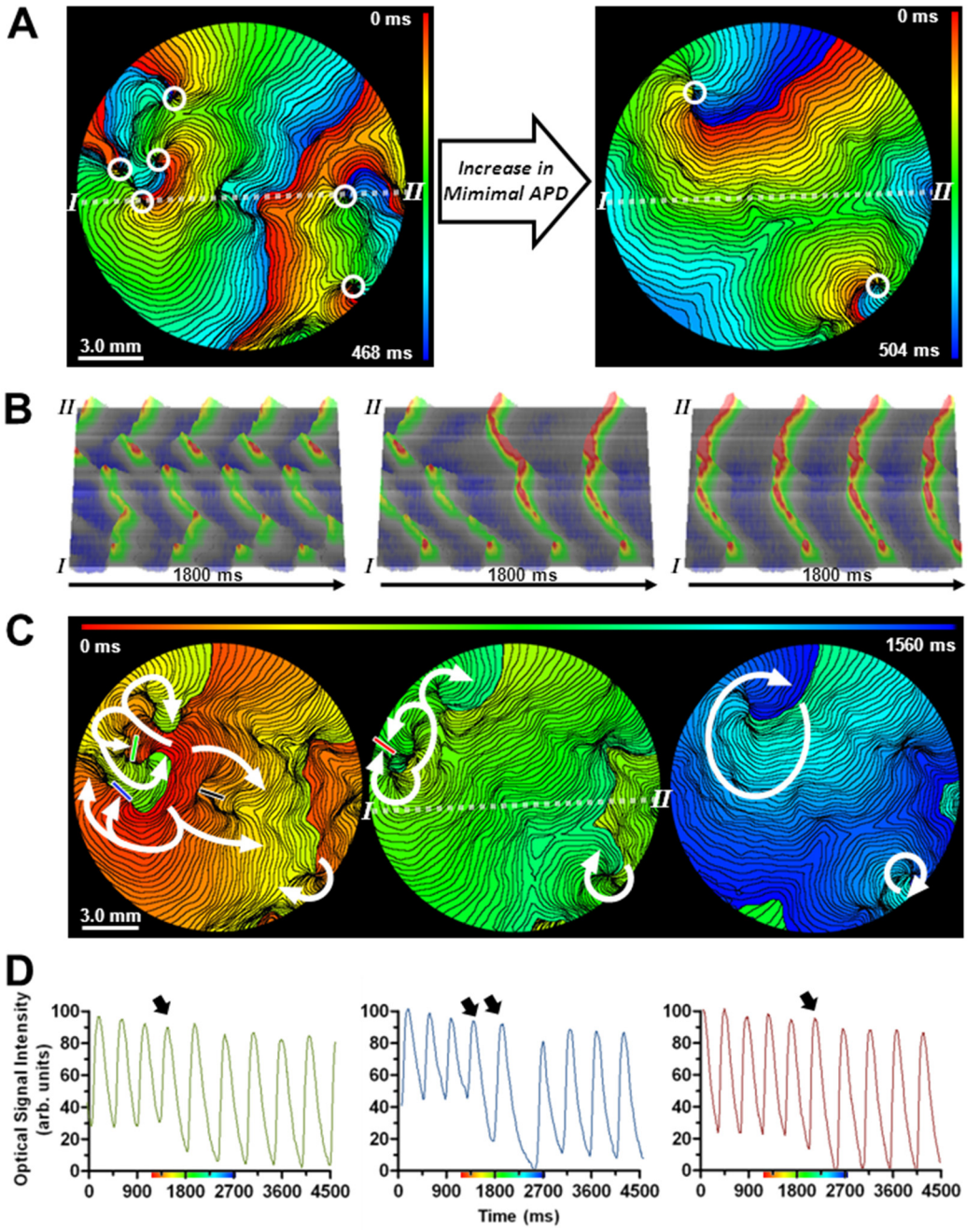

Figure 5. *(A) Activation maps of a culture treated with 20μM 2-APB, before (left) and after (right) minimal APD prolongation. White circles indicate rotor position. (B) Examples of 3 consecutive 3D (rotated 15º) line scan analyses, during 1800 s, from point I to point II in culture shown in A, before (left), during (center) and after (right) minimal APD prolongation. (C) Consecutive activation maps*

during rotor termination by APD prolongation. The green, blue, black and red bars indicate the area of critical wave front collision. (D) Optical action potentials at the areas of critical wave front collision of corresponding colors shown in C. Black arrows mark the moment of critical wave front collision.

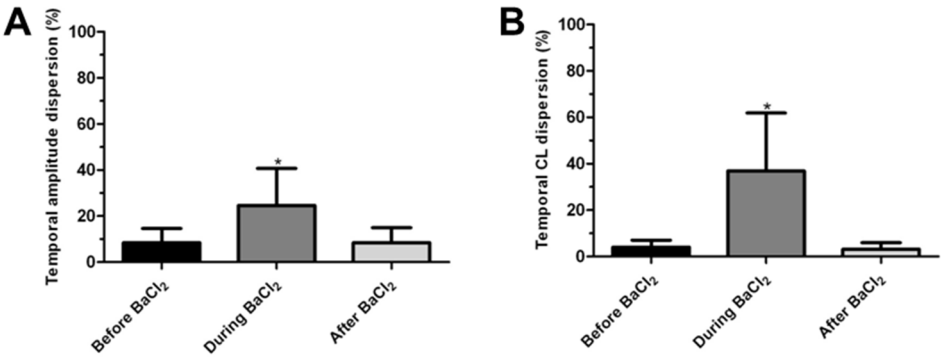

Supplemental Figure 4. *Increasing minimal APD by $BaCl_2$ causes transient instability in optical signal amplitude and rotor cycle length. (A) Quantification of temporal dispersion of optical signal amplitude and (B) temporal dispersion of rotor cycle length, prior to, during and after increasing minimal APD by the incubation with $BaCl_2$. *:P<0.05 vs. before $BaCl_2$.*

2-APB in adult rat heart ventricles

To investigate the functional implications of *in vitro* findings on the intact heart, Langendorff-perfused adult rat hearts were subjected to *ex vivo* optical mapping. Baseline activation frequency before addition of BDM to the oxygenated Tyrode perfusate was 4.50±0.5Hz. After addition of BDM sinus rhythm remained stable for at least 1 hour at an average activation frequency of 2.5±0.4Hz (Supplemental Figure 5A and 5B). Perfusion with oxygenated Tyrode supplemented with 5µmol/L 2-APB for 20 minutes slowed conduction from 54.1±3.2cm/s to 27.8±2.7cm/s (n=6, P<0.05). No arrhythmias developed at this dosage and sinus rhythm was maintained at 2.5±0.5Hz (Supplemental Figure 5A-C, P>0.05 vs. control). Perfusion of hearts with 10 µmol/L 2-APB caused VT in all hearts (2.2±0.2 wave fronts at 5.4±3.3Hz, n=6), whereas complexity of arrhythmias increased to fibrillation with 20µmol/L 2-APB (5.0±1.1 wave fronts at 11.0±0.9Hz, n=6) (Supplemental Figure 5A and 5C). Complexity of arrhythmias stabilized within 10 minutes of incubation with 2-APB.

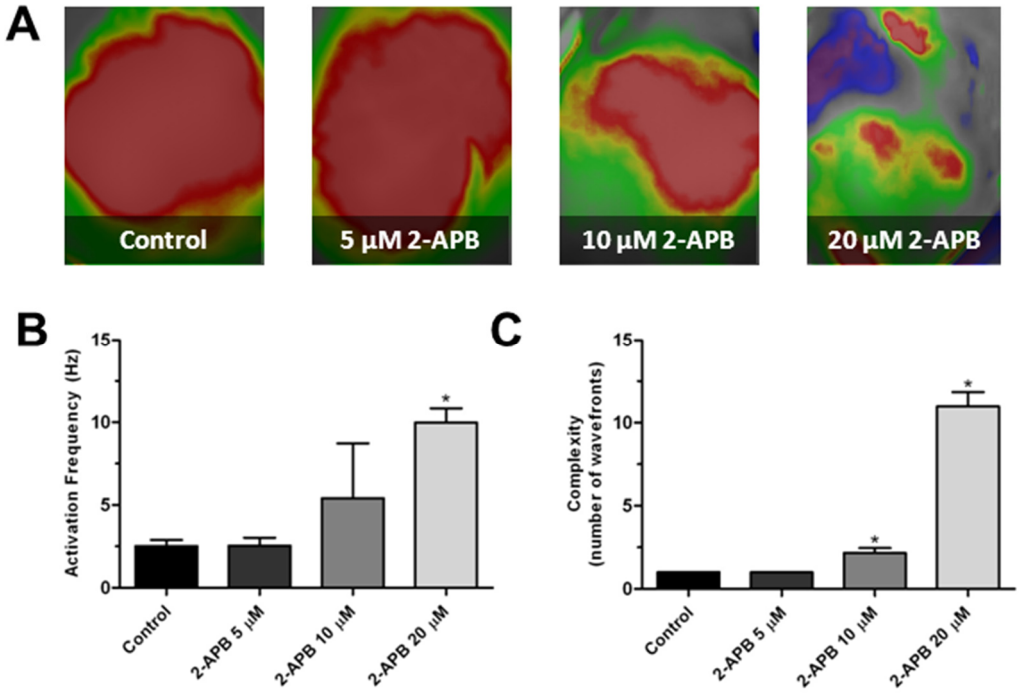

Supplemental Figure 5. *A 2-APB dose-dependent increase in arrhythmia complexity in adult Wistar rat hearts leading to sustained VF. (A) Typical snapshots of ventricular activation during optical mapping of Langendorff-perfused adult rat heart perfused with (from left to right) normal Tyrode solution and tyrode solution supplemented with 5, 10 and 20 µM 2-APB. (B) Quantification of average activation frequency and (C) complexity in control hearts, and hearts treated with 2-APB. *: P<0.05 vs control*

Minimal APD determines arrhythmia complexity in adult rat heart ventricles

To investigate whether $BaCl_2$ lowered arrhythmia complexity ex vivo as in vitro, rat hearts were first perfused with 20mmol/L 2-APB until fibrillation was present and stable for at least 5 min. Then, 500 mmol/L of $BaCl_2$ was added to the perfusate consisting of tyrode with 20mmol/L 2-APB. Typically within 5 min, $BaCl_2$ decreased arrhythmia complexity by 71.4% compared with controls (Figure 6A, C, and D, n = 6). Also, activation frequency decreased from 9.98+0.9 to 2.8+0.3 Hz by $BaCl_2$ (Figure 6A and C). Importantly, $BaCl_2$ treatment significantly increased minimal APD80 to 265.4+35.1% of control hearts (Figure 6B, n = 6). Together these results show that, similar to in vitro experiments, arrhythmia complexity can be decreased by increasing minimal APD ex vivo.

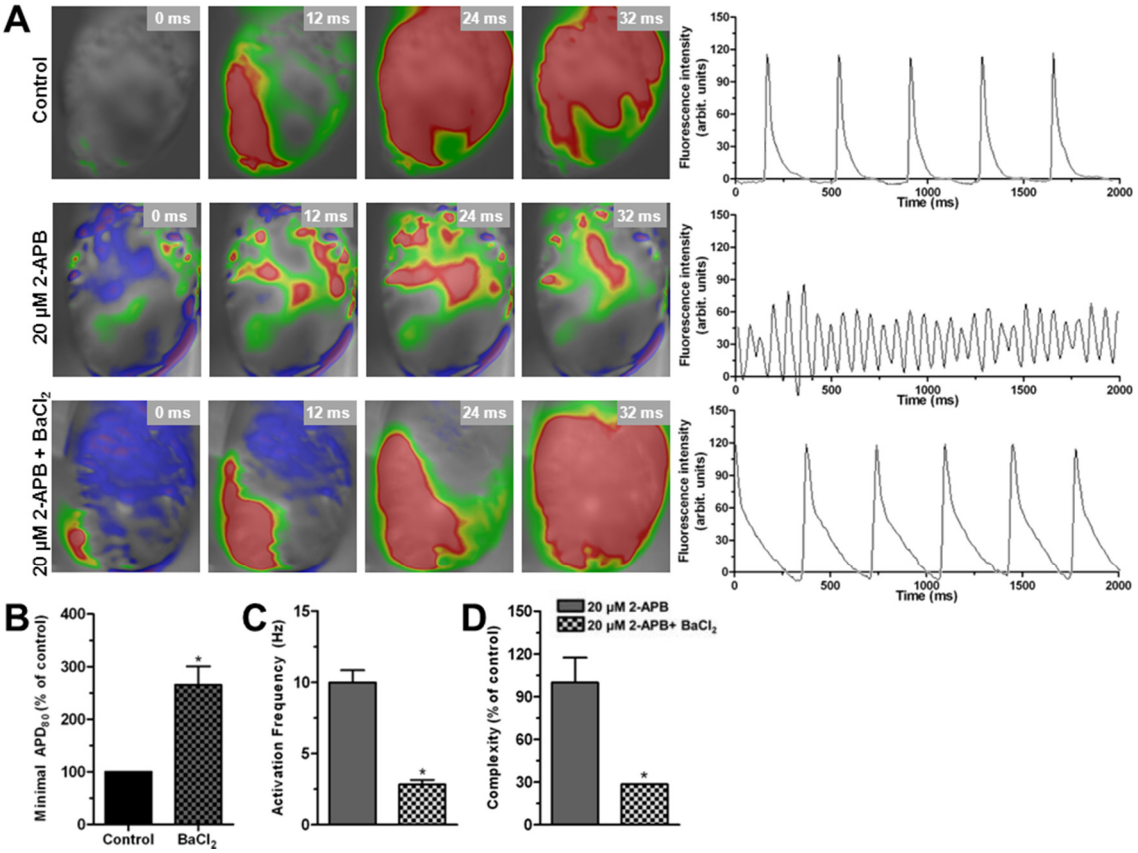

Figure 6. *(A) Typical sequence (12ms between snapshots) of activation in (from top to bottom) Langendorff-perfused control hearts, 20µM 2-APB treated hearts, and 20µM 2-APB treated hearts after introduction of $BaCl_2$ with corresponding optical action potential signals. (B) Quantification of minimal APD in control hearts and hearts perfused with 500µmol/L $BaCl_2$. (C) Assessment of activation frequency and (D) complexity in hearts treated with 20µM 2-APB before and after introduction of $BaCl_2$. *: P<0.05 vs. control.*

Discussion

The key findings of this study are (1) incubation with 2-APB induces reentrant tachyarrhythmias in myocardial cultures and adult rat hearts, which are maintained by multiple stable and co-existing rotors, resembling sustained VF. (2) The complexity of these arrhythmias increases exponentially with increasing dosages of 2-APB, allowing a systematic study of arrhythmia complexity *in vitro* and *ex vivo*. (3) Increasing arrhythmia complexity during fibrillation is associated with a shortening of the average wavelength and APD. (4) Hence, complexity and activation frequency during fibrillation could be decreased pharmacologically by transient destabilization of sustained VF through prolongation of minimal APD *in vitro* and *ex vivo*, regardless of ionic mechanism.

The importance of wavelength in reentrant tachyarrhythmias

Since the introduction of the circus movement reentry theory[23] and the leading circle concept,[24] it has been established that if the wavelength of a given reentrant circuit exceeds the path-length, reentry cannot be sustained as a consequence of a vanishing excitable gap. Hence, wavelength prolongation has traditionally been viewed as an important anti-arrhythmic strategy.[12,13] Elaborating on this theory, we now demonstrated that wavelength prolongation affects co-existence of multiple neighboring rotors, although rotor termination by prolongation of wavelength in single rotor tachyarrhythmias appeared to be more complicated (Figure 4D; 10µmol/L 2-APB). The slope in the relationship between wavelength and complexity is steepest in the low complexity range (<2 rotors) (Figure 2D). This implies that in the lower complexity range a greater wavelength prolongation is necessary to facilitate the same decrease in complexity. Also, the absence of boundaries formed by neighboring rotors diminishes the chance of rotor termination in the lower complexity range. Moreover, we show that the effect of a given agent on arrhythmia complexity depends on the activity of the agent at high frequency activation, which can differ from its effect at low frequencies. Sotalol, for instance had a significant effect on 1Hz APD, but not on minimal APD , which may explain the inability of sotalol to terminate rotors during VF. In contrast, increasing minimal APD by $BaCl_2$ and BayK8644, induced a notable reduction in the number of rotors during VF. However, decreasing minimal APD by nitrendipine treatment did not increase average arrhythmia complexity. This can be explained by the minute tendency for the formation of new wave breaks during sustained VF, despite an increase in effective size of the culture.

Importantly, in earlier *in silico* work by Ten Tusscher *et al*., minimal APD was shown to be predictive of arrhythmia complexity in animal and human hearts.[25,26] We now showed that minimal APD is not only predictive of arrhythmia complexity, but that prolongation of minimal APD also strongly and effectively reduced arrhythmia complexity.

APD and CV restitution in fibrillation

Other theories involving prevention or termination of VF mostly originate from the 'multiple wavelet' and the 'mother rotor' theory.[16,27] In general, both assume flattening of APD restitution or narrowing of CV restitution should prevent wave breaks and consequent disorganization of conduction, which should result in termination of VF.[16,27] Indeed, several studies confirmed that flattening of APD restitution by for instance verapamil or bretylium can convert VF to VT.[10,11,14,28]

However, the anti-fibrillatory effects of aforementioned substances are generally confirmed by mapping or *in silico* models during or resembling the first minute after VF induction. Yet, Wiggers *et al*. showed that the heart goes through several stages during VF,[9] by which organization and periodicity increase after the first 2 min.[6-8,10] Hence, therapies aiming to decrease disorganization of conduction could prove to be effective only in this first phases of fibrillation. The findings in the present study partially explain Wiggers' stages III and IV of fibrillation because as ischemia progresses, gap junctional coupling is reduced which may slow VF into a stable, organized and periodical multi-rotor arrhythmia. Our data on these typical characteristics of sustained VF are consistent with a previous report of sustained (slow) VF in an isolated rabbit heart model of VF.[10] Furthermore, we showed that during these phases of VF, interventions that flatten APD or CV restitution in an attempt to terminate VF may be considered inadequate. This is best exemplified by the effect of the I_{CaL} inhibitor nitrendipine on VF after 2-APB treatment, which according to earlier studies should have flattened APD restitution and terminated VF. However, nitrendipine only caused detrimental effects: increasing activation frequency without affecting complexity. Interestingly, activation of I_{CaL}, by BayK8644 treatment, did decrease complexity during VF, exemplifying the reversal of effects of I_{CaL} targeting in the early phases through the later phases of VF.

I_{K1} blockade and VF termination

Another approach to revert sustained VF to VT or sinus rhythm could be to destabilize the rotors maintaining VF in an effort to achieve termination of these rotors by collision with a preexisting boundary.[15,29] In several studies rotor stability was demonstrated to depend on specific ion channel currents, such as I_{K1}.[14,15,29-31] We showed that blockade of I_{K1} during VF decreased rotor frequency and the complexity of conduction, ultimately reverting VF back to VT.[32] However, rotor stability during VF did not seem to be specifically dependent on the I_{K1} current but on the effect blockade of I_{K1} had on the minimal APD. Therefore, the decrease in complexity could be reproduced with Bayk8644, a substance that increases minimal APD by augmenting I_{CaL}, without affecting I_{K1}.[33] By altering the stability of these rotors, collision of rotors with preexisting boundaries, but also novel critical boundaries formed by wave fronts propagated from adjacent rotors are enforced, significantly reducing the complexity of activation patterns during fibrillation.

Patients suffering from sustained VF are still in a timeframe to be resuscitated without cerebral damage.[34] Therefore, the observation that an increase in minimal APD decreases complexity of sustained VF may have important consequences for the treatment of VF, since VF, when driven by a smaller number of rotors, requires less energy for defibrillation.[35]

Study limitations

In our study, 2-APB treatment was used to induce arrhythmias. This agent is known to block gap junctional communication, but also the IP3 receptor and TRP channels, while causing activation of voltage- independent calcium channels.[18,19,36] Of these effects, gap junctional uncoupling has been shown to be related to arrhythmia induction in CMC cultures as a consequence of wave breaks caused by preexistent heterogeneity in gap junctional coupling.[2,37,38] In addition, voltage-independent calcium influx may also cause pro-arrhythmic features in 2-APB treated hearts.[36] As such, the clinical significance of these mechanisms of VF initiation may be very limited. However, as VF can show the same maintenance properties, regardless of the method of initiation[39], this does not hinder the study of VF maintenance and termination as was performed in the present study.

In the *ex vivo* mapping experiments, complexity was determined by the number of epicardial wave fronts, instead of the number of rotors. However, in line with previous research we found that during sustained VF, the number of epicardial rotors is minimal, attenuating the significance of the epicardial number of rotors.[10]

Moreover, this study makes use of a neonatal rat cardiomyocyte culture model as well as adult rat hearts. Rat hearts differ considerably from human hearts in terms of the ion currents determining the action potential morphology. Hence, the conclusions drawn from this study are only conceptual in relation to the mechanisms of ventricular fibrillation maintenance and cannot be readily extrapolated to the human or clinical setting.

Conclusions

Incubation of neonatal rat myocardial cultures or Langendorff-perfused adult rat hearts with increasing dosage of 2-APB allows for the systematic study of arrhythmia complexity, ultimately resembling sustained VF. Arrhythmia complexity and activation frequency during fibrillation can be decreased pharmacologically by transient VF destabilization through prolongation of minimal APD *in vitro* and *ex vivo*, regardless of ionic mechanism. Accordingly, this study could provide a novel conceptual framework for future anti-arrhythmic drug design as well as an extension in the rationale for treatment options of sustained VF.

Funding
This work was supported by the Netherlands Organisation for Scientific Research (NWO; VENI grant [91611070 to D.A.P], the Dutch Heart Foundation [2008/B119], the Fund for Scientific Research Flanders (FWO grant [G084811N to I.V.K. and A.V.P.]) and Institut des Hautes Etudes Scientifiques, Bures-sur-Yvette, France, and to the James Simons Foundation [I.V.K.].

Acknowledgements
We wish to thank Wilbert P.M van Meerwijk, PhD for helpful discussions, Adriana C. Gittenberger-de Groot, PhD for helpful comments on the manuscript, and Huybert J.F. van der Stadt and Gerry T.M. Wagenaar, PhD for excellent technical and scientific support.

Conflict of interest
None declared.

Supplemental Material

Methods

All animal experiments were approved by the Animal Experiments Committee of the Leiden University Medical Center and conform to the Guide for the Care and Use of Laboratory Animals as stated by the US National Institutes of Health.

Cell Isolation and culture

Neonatal rat ventricular myocytes were isolated by collagenase digestion as described previously.[17] Briefly, animals were anaesthetized with 4–5% isoflurane inhalation anesthesia.

Adequate anesthesia was assured by the absence of reflexes prior to rapid heart excision.

After animal sacrifice by rapid heart excision, ventricles were minced and digested using collagenase (Worthington, Lakewood, NJ, USA) and DNAse (Sigma-Aldrich, St. Louis, MO, USA). Cell suspensions from a 50 minutes and a subsequent 45 minutes dissociation were pooled, centrifuged and resuspended in HAM's F10 medium supplemented with 10% fetal bovine serum and 10% horse serum (HS) (Invitrogen, Carlsbad, CA, USA). Cells were preplated on Primaria coated culture dishes (BD Biosciences, Franklin Lakes, NJ, USA) to allow preferential attachment of cardiac fibroblasts. Subsequently, cell aggregates and debris were removed by filtering non-adherent cells through a 70 µM cell strainer. Following isolation myocardial cells were plated out on fibronectin-coated, round glass coverslips (15 mm) at a cell density of 2-8x10^5 cells/well in 24-well plates (Corning Life Sciences, Amsterdam, the Netherlands) depending on the experiment. To prevent overgrowth of remaining cardiac fibroblasts, proliferation was inhibited by Mitomycin-C (Sigma) treatment at day 1, as described previously.[17] All cultures were refreshed daily with DMEM/HAM's F10 in a 1:1 mixture with 5% HS and cultured in a humidified incubator at 37º C and 5% CO_2.

Immunocytological analyses

Cultures were stained for Connexin40 (Santa Cruz Biotechnologies, Santa Cruz, CA, USA) connexin43 (Sigma), and connexin45 (Santa Cruz) to assess presence of gap junctional proteins, and for active caspase-3 (Abcam, Cambridge, MA, USA) to assess the number of apoptotic cells. For this purpose, cells were fixated in 1% paraformaldehyde in PBS and permeabilized with 0.1% Triton X-100 in PBS. Primary antibodies and corresponding secondary Alexa fluor-conjugated antibodies (Invitrogen) were used at a 1:200 dilution. Counterstaining of nuclei was performed with Hoechst 33342 (Invitrogen). Images of cultures were taken and quantified using dedicated software (ImageJ, National Institutes of Health, USA).

Whole-cell patch-clamp

Whole-cell measurements were performed in spontaneously active cultures plated out in a density of $4x10^5$ cells/well in 24 well plates. At day 4 of culture, current-clamp experiments were performed in CMCs at 25° C using an L/M-PC patch-clamp amplifier (3 kHz filtering) (List-Medical, Darmstadt, Germany). The pipette solution contained (in mmol/L) 10 Na_2ATP, 115 KCl, 1 $MgCl_2$, 5 EGTA, 10 HEPES/KOH (pH 7.4). To study the effects of gap junctional uncoupling by 2-APB on electrophysiological properties of CMCs, 25 µM 2-APB (Tocris Bioscience, Bristol, United Kingdom) was incubated for 20 minutes prior to measurements.[17,40]

Tip and seal resistance were 2.0-2.5 MΩ and >1 GΩ, respectively. The bath solution contained (in mmol/L) 137 NaCl, 4 KCl, 1.8 $CaCl_2$, 1 $MgCl_2$, and 10 HEPES (pH 7.4). For data acquisition and analysis, pClamp/Clampex8 software (Axon Instruments, Molecular Devices, Sunnyvale, CA, USA) was used.

Optical mapping

At day 4 of culture, propagation of action potentials was investigated on a whole-culture scale by optical mapping using di-4-anepps as voltage sensitive dye, as described previously.[17] Structurally inhomogeneous cultures, as judged by light microscopy and mapping, were excluded for reasons of reproducibility and standardization (90 out of every 100 cultures were included). CMC cultures were plated out in 24-well plates (Corning) at a cell density of $8x10^5$ cells per well. Cultures underwent daily refreshing of culture medium and >2 hours prior to mapping, after which cultures were incubated with serum-free DMEM and colorless HAM's F10 in a 1:1 mixture (mapping medium), with 8 µmol/L di-4-anepps (Sigma) for 15±5 minutes at 37º C in a humidified incubator. Subsequently, cultures were refreshed with mapping medium. Cells were incubated with 2-APB dissolved in DMSO in 5 different concentrations (5, 10, 15, 20 and 25 µM) for 20±2 min in mapping medium, targeting Connexin43, Connexin45 and Connexin40 to induce gap junctional uncoupling,[18,19] while vehicle treated cultures were used as controls. Next, electrical propagation patterns were recorded by optical mapping at 37º C. Mapping experiments typically did not exceed 20 minutes per 24-wells plate. Also, cultures were not exposed to excitation light for longer than 40 s to limit possible phototoxic effects. Excitation light (e_{ex}=525±25 nm) was delivered by a halogen arc-lamp (MHAB-150W, Moritex Corporation, San Jose, CA, USA) through epi-illumination. Fluorescent emission light passed through a dichroic mirror and a long-pass emission filter (>590 nm) and was focused onto a 100x100 pixels CMOS camera (Ultima-L, SciMedia, Costa Mesa, CA, USA) by a 1.6x converging lens (Leice, Wetzlar, Germany). This resulted in a spatial resolution of 160 µm/pixel and a field of view of 16 by 16 mm. Spontaneous or stimulated electrical activity was recorded for 6-24 s at 6 ms exposure time per frame. Data analysis, construction of activation maps and stripe analysis (e.g. plotting

of optical signal amplitude against time, at the maximal diameter of a culture or short and long axis of whole heart) were performed with specialized software (Brainvision Analyze 1101, Brainvision Inc, Tokyo, Japan) after pixel signals were averaged with 8 of its nearest neighbors, minimizing noise-artifacts. Conduction velocity (CV), action potential duration until 80% repolarization (APD_{80}) and activation frequency were determined at six different locations equally distributed throughout the culture and averaged before further analysis. Wavelength was calculated by the product of average CV and APD_{80} (for uniform propagation) or reentrant cycle length.[12] Temporal dispersion of optical signal amplitude was defined as the difference between the minimal and the maximal optical signal amplitude (in arbitrary units) within 6 s of mapping, expressed as a percentage of the minimal optical signal amplitude. Temporal dispersion of reentrant cycle length was defined as the difference between the minimal and the maximal reentrant cycle length (in ms) within 6 s of mapping, expressed as a percentage of the minimal reentrant cycle length.

Assessment and modification of 1 Hz and minimal APD

As a result of the outcome of correlating changes in APD and wavelength with arrhythmia complexity, the effect of several ion channel modulators on APD was tested during low and high-frequency activation. This was necessary to study the effect of ion channel activation and inactivation dynamics during normal versus rapid activation on the outcome of pharmacological ion channel modulation on APD. For this purpose, we used a custom-made epoxy-coated platinum electrode and performed supra-threshold, 10 ms duration, square, unipolar stimulation using an electrical stimulus module with corresponding software (Multichannel Systems, Reutlingen, Germany). Using this electrode, cultures were paced at 1-10 Hz with 1 Hz increments. Minimal APD was defined as the APD_{80} determined at the pacing frequency (1-10 Hz) resulting in the shortest possible diastolic interval for that specific culture. Ion channel modulation was performed by administering specific ion channel modulators (which according to their mechanism of action should have an effect on APD) directly into the mapping medium and dispersing them by gentle agitation. To reduce the Ca^{2+} influx, L-type Ca^{2+} inward current (I_{CaL}) was inhibited by administration of nitrendipine (3 µmol/L) (Sigma) to reduce APD. Sotalol (1mM) (Sigma), 0.5mM $BaCl_2$ (Merck, Darmstadt, Germany), inhibiting the inward rectifier the current and BayK8644 (1 µmol/L) (Sigma) increasing the I_{CaL}, were used to increase APD. Cultures were optically mapped prior to and after 10s incubation with these pharmacological agents

During *ex vivo* experiments in adult rat hearts, APD_{80} was measured during 3 s of pacing with a unipolar platinum electrode at 1-10 Hz, to determine minimal APD. To assess the effect of $BaCl_2$ on minimal APD *ex vivo*, 500 µmol/L $BaCl_2$ was added to the perfusate for 5 minutes prior to determination of minimal APD.

Pharmacological interventions during VF

To investigate the effects of APD modifications on VF characteristics, the above mentioned pharmacological agents were also administered to 2-APB treated and control cultures. Cultures were optically mapped before and after 10 s of incubation.

In experiments involving agents that reduced VF complexity, optical signals were recorded through a transparent, permeable membrane (0.4 µm pore size) (Corning) placed in the solution above the culture that allowed for a slow and even distribution of the agents. Using this method the actual process of complexity reduction could be visualized and its underlying mechanisms could be analyzed.

During *ex vivo* experiments, after initiation of VF by 10 minutes perfusion of 20 µmol/L 2-APB, 500 µmol/L $BaCl_2$ was added to the perfusate for 10 minutes prior to measurements to study its effects on arrhythmia complexity. Importantly, the perfusate contained 2-APB prior to and during $BaCl_2$ perfusion to prevent washout of 2-APB.

Supplemental Results

2-APB dosage	APD_{80} (% of control); p value vs control			
	Nitrendipine	**Sotalol**	**$BaCl_2$**	**BayK8644**
10 µM	73±12%; *P*<0.01	107±3%; *P*=ns	167±28%; *P*<0.05	140±19%; *P*<0.05
15 µM	77±8%; *P*<0.001	105±6%; *P*=ns	159±27%; *P*<0.001	154±25%; *P*<0.01
20 µM	73±10%; *P*<0.0001	110±6%; *P*=ns	179±38%; *P*<0.0001	150±20%; *P*<0.001
25 µM	77±10%; *P*<0.01	112±11%; *P*=ns	149±10%; *P*<0.0001	155±13%; *P*<0.0001

Supplemental Table 1. APD_{80} values after pharmacological ion channel modulation by nitrendipine, sotalol, $BaCl_2$ or BayK8644 during 2-APB (10-25 µM) induced fibrillation. Controls are set at 100%. ns: non-significant.

2-APB dosage	Wavelength (% of control); p value vs control			
	Nitrendipine	**Sotalol**	**$BaCl_2$**	**BayK8644**
10 µM	87±7%; *P*<0.01	105±9%; *P*=ns	131±37%; *P*<0.05	126±24%; *P*<0.05
15 µM	85±16%; *P*=ns	95±23%; *P*=ns	155±28%; *P*<0.001	153±44%; *P*<0.05
20 µM	94±14%; *P*=ns	110±18%; *P*=ns	163±54%; *P*<0.001	160±40%; *P*<0.01
25 µM	89±13%; *P*=ns	111±15; *P*=ns	150±20%; *P*<0.01	150±23%; *P*<0.001

Supplemental Table 2. Wavelength values after pharmacological ion channel modulation by nitrendipine, sotalol, $BaCl_2$ or BayK8644 during 2-APB (10-25 µM) induced fibrillation. Controls are set at 100%. ns: non-significant.

2-APB dosage	Activation frequency (% of control); p value vs control			
	Nitrendipine	**Sotalol**	**$BaCl_2$**	**BayK8644**
10 µM	113±6%; *P*<0.01	95±6%; *P*=ns	75±16%; *P*<0.05	75±9%; *P*<0.01
15 µM	112±11%; *P*<0.05	94±4%; *P*<0.05	67±11%; *P*<0.0001	66±13%; *P*<0.001
20 µM	117±6%; *P*<0.0001	92±6%; *P*<0.05	55±19%; *P*<0.0001	73±8%; *P*<0.0001
25 µM	112±11%; *P*<0.05	93±9%; *P*=ns	69±7%; *P*<0.0001	69±5%; *P*<0.0001

Supplemental Table 3. Activation frequency values after pharmacological ion channel modulation by nitrendipine, sotalol, $BaCl_2$ or BayK8644 during 2-APB (10-25 µM) induced fibrillation. Controls are set at 100%. ns: non-significant.

2-APB dosage	Complexity (% of control); p value vs control			
	Nitrendipine	**Sotalol**	**$BaCl_2$**	**BayK8644**
10 µM	100±0%; *P*=ns	100±0%; *P*=ns	89±19%; *P*=ns	83±41%; *P*=ns
15 µM	111±17%; *P*=ns	108±20%; *P*=ns	73±25%; *P*<0.05	56±22%; *P*<0.01
20 µM	99±15%; *P*=ns	102±14; *P*=ns	30±22%; *P*<0.0001	43±15%; *P*<0.0001
25 µM	102±9%; *P*=ns	87±7%; *P*<0.01	52±11%; *P*<0.0001	37±11%; *P*<0.0001

Supplemental Table 4. Complexity values after pharmacological ion channel modulation by nitrendipine, sotalol, $BaCl_2$ or BayK8644 during 2-APB (10-25 µM) induced fibrillation. Controls are set at 100%. ns: non-significant

References

1. Zipes DP and Wellens HJ. Sudden cardiac death. *Circulation*. 1998;98:2334-2351.

2. Huikuri HV, Castellanos A, Myerburg RJ. Sudden death due to cardiac arrhythmias. *N Engl J Med*. 2001;345:1473-1482.

3. Severs NJ, Bruce AF, Dupont E, Rothery S. Remodelling of gap junctions and connexin expression in diseased myocardium. *Cardiovasc Res*. 2008;80:9-19.

4. Weiss JN, Qu Z, Chen PS, Lin SF, Karagueuzian HS, Hayashi H, Garfinkel A, Karma A. The dynamics of cardiac fibrillation. *Circulation*. 2005;112:1232-1240.

5. Gutstein DE, Morley GE, Tamaddon H, Vaidya D, Schneider MD, Chen J, Chien KR, Stuhlmann H, Fishman GI. Conduction slowing and sudden arrhythmic death in mice with cardiac-restricted inactivation of connexin43. *Circ Res*. 2001;88:333-339.

6. Clayton RH, Nash MP, Bradley CP, Panfilov AV, Paterson DJ, Taggart P. Experiment-model interaction for analysis of epicardial activation during human ventricular fibrillation with global myocardial ischaemia. *Prog Biophys Mol Biol*. 2011;107:101-111.

7. Huang J, Rogers JM, Killingsworth CR, Singh KP, Smith WM, Ideker RE. Evolution of activation patterns during long-duration ventricular fibrillation in dogs. *Am J Physiol Heart Circ Physiol*. 2004;286:H1193-H1200.

8. Kleber AG, Riegger CB, Janse MJ. Electrical uncoupling and increase of extracellular resistance after induction of ischemia in isolated, arterially perfused rabbit papillary muscle. *Circ Res*. 1987;61:271-279.

9. Wiggers CJ, Bell JR, Paine M. Studies of ventricular fibrillation caused by electric shock: II. Cinematographic and electrocardiographic observations of the natural process in the dog's heart. Its inhibition by potassium and the revival of coordinated beats by calcium. *Ann Noninvasive Electrocardiol*. 2003;8:252-261.

10. Wu TJ, Lin SF, Weiss JN, Ting CT, Chen PS. Two types of ventricular fibrillation in isolated rabbit hearts: importance of excitability and action potential duration restitution. *Circulation*. 2002;106:1859-1866.

11. Garfinkel A, Kim YH, Voroshilovsky O, Qu Z, Kil JR, Lee MH, Karagueuzian HS, Weiss JN, Chen PS. Preventing ventricular fibrillation by flattening cardiac restitution. *Proc Natl Acad Sci U S A*. 2000;97:6061-6066.

12. Panfilov AV. Is heart size a factor in ventricular fibrillation? Or how close are rabbit and human hearts? *Heart Rhythm*. 2006;3:862-864.

13. Rensma PL, Allessie MA, Lammers WJ, Bonke FI, Schalij MJ. Length of excitation wave and susceptibility to reentrant atrial arrhythmias in normal conscious dogs. *Circ Res*. 1988;62:395-410.

14. Samie FH, Mandapati R, Gray RA, Watanabe Y, Zuur C, Beaumont J, Jalife J. A mechanism of transition from ventricular fibrillation to tachycardia : effect of calcium channel blockade on the dynamics of rotating waves. *Circ Res*. 2000;86:684-691.

15. Warren M, Guha PK, Berenfeld O, Zaitsev A, Anumonwo JM, Dhamoon AS, Bagwe S, Taffet SM, Jalife J. Blockade of the inward rectifying potassium current terminates ventricular fibrillation in the guinea pig heart. *J Cardiovasc Electrophysiol*. 2003;14:621-631.

16. Zaitsev AV, Berenfeld O, Mironov SF, Jalife J, Pertsov AM. Distribution of excitation frequencies on the epicardial and endocardial surfaces of fibrillating ventricular wall of the sheep heart. *Circ Res*. 2000;86:408-417.

17. Askar SF, Ramkisoensing AA, Schalij MJ, Bingen BO, Swildens J, van der Laarse A, Atsma DE, de Vries AA, Ypey DL, Pijnappels DA. Antiproliferative treatment of myofibroblasts prevents arrhythmias in vitro by limiting myofibroblast-induced depolarization. *Cardiovasc Res*. 2011;90:295-304.

18. Bai D, del CC, Srinivas M, Spray DC. Block of specific gap junction channel subtypes by 2-aminoethoxydiphenyl borate (2-APB). *J Pharmacol Exp Ther*. 2006;319:1452-1458.

19. Harks EG, Camina JP, Peters PH, Ypey DL, Scheenen WJ, van Zoelen EJ, Theuvenet AP. Besides affecting intracellular calcium signaling, 2-APB reversibly blocks gap junctional coupling in confluent monolayers, thereby allowing measurement of single-cell membrane currents in undissociated cells. *FASEB J*. 2003;17:941-943.

20. Gray RA, Pertsov AM, Jalife J. Spatial and temporal organization during cardiac fibrillation. *Nature*. 1998;392:75-78.

21. Nash MP, Mourad A, Clayton RH, Sutton PM, Bradley CP, Hayward M, Paterson DJ, Taggart P. Evidence for multiple mechanisms in human ventricular fibrillation. *Circulation*. 2006;114:536-542.

22. Kleber AG and Rudy Y. Basic mechanisms of cardiac impulse propagation and associated arrhythmias. *Physiol Rev*. 2004;84:431-488.

23. Mines GR. On dynamic equilibrium in the heart. *J Physiol*. 1913;46:349-383.

24. Allessie MA, Bonke FI, Schopman FJ. Circus movement in rabbit atrial muscle as a mechanism of trachycardia. *Circ Res*. 1973;33:54-62.

25. ten Tusscher KH, Mourad A, Nash MP, Clayton RH, Bradley CP, Paterson DJ, Hren R, Hayward M, Panfilov AV, Taggart P. Organization of ventricular fibrillation in the human heart: experiments and models. *Exp Physiol*. 2009;94:553-562.

26. ten Tusscher KH, Hren R, Panfilov AV. Organization of ventricular fibrillation in the human heart. *Circ Res*. 2007;100:e87-101.

27. Moe GK and ABILDSKOV JA. Atrial fibrillation as a self-sustaining arrhythmia independent of focal discharge. *Am Heart J*. 1959;58:59-70.

28. Riccio ML, Koller ML, Gilmour RF, Jr. Electrical restitution and spatiotemporal organization during ventricular fibrillation. *Circ Res*. 1999;84:955-963.

29. Sekar RB, Kizana E, Cho HC, Molitoris JM, Hesketh GG, Eaton BP, Marban E, Tung L. IK1 heterogeneity affects genesis and stability of spiral waves in cardiac myocyte monolayers. *Circ Res*. 2009;104:355-364.

30. Jalife J. Inward rectifier potassium channels control rotor frequency in ventricular fibrillation. *Heart Rhythm*. 2009;6:S44-S48.

31. Tsuchihashi K and Curtis MJ. Influence of tedisamil on the initiation and maintenance of ventricular fibrillation: chemical defibrillation by Ito blockade? *J Cardiovasc Pharmacol*. 1991;18:445-456.

32. Rees SA and Curtis MJ. Specific IK1 blockade: a new antiarrhythmic mechanism? Effect of RP58866 on ventricular arrhythmias in rat, rabbit, and primate. *Circulation*. 1993;87:1979-1989.

33. Yatani A, Kunze DL, Brown AM. Effects of dihydropyridine calcium channel modulators on cardiac sodium channels. *Am J Physiol*. 1988;254:H140-H147.

34. Safar P. Cerebral resuscitation after cardiac arrest: research initiatives and future directions. *Ann Emerg Med*. 1993;22:324-349.

35. Hillebrenner MG, Eason JC, Trayanova NA. Mechanistic inquiry into decrease in probability of defibrillation success with increase in complexity of preshock reentrant activity. *Am J Physiol Heart Circ Physiol*. 2004;286:H909-H917.

36. Wang P, Umeda PK, Sharifov OF, Halloran BA, Tabengwa E, Grenett HE, Urthaler F, Wolkowicz PE. Evidence that 2-aminoethoxydiphenyl borate provokes fibrillation in perfused rat hearts via voltage-independent calcium channels. *Eur J Pharmacol*. 2012;681:60-67.

37. Nakagami T, Tanaka H, Dai P, Lin SF, Tanabe T, Mani H, Fujiwara K, Matsubara H, Takamatsu T. Generation of reentrant arrhythmias by dominant-negative inhibition of connexin43 in rat cultured myocyte monolayers. *Cardiovasc Res*. 2008;79:70-79.

38. Bub G, Shrier A, Glass L. Spiral wave generation in heterogeneous excitable media. *Phys Rev Lett*. 2002;88:058101.

39. Curtis MJ and Hearse DJ. Ischaemia-induced and reperfusion-induced arrhythmias differ in their sensitivity to potassium: implications for mechanisms of initiation and maintenance of ventricular fibrillation. *J Mol Cell Cardiol*. 1989;21:21-40.

40. Pijnappels DA, Schalij MJ, Ramkisoensing AA, van Tuyn J, de Vries AA, van der Laarse A, Ypey DL, Atsma DE. Forced alignment of mesenchymal stem cells undergoing cardiomyogenic differentiation affects functional integration with cardiomyocyte cultures. *Circ Res*. 2008;103:167-176.